

Journal Pre-proof

Charge-enhanced thiourea catalysts as hydrogen bond donors for Friedel–Crafts Alkylations

Ivor Smajlagic, Brenden Carlson, Nicholas Rosano, Hayden Foy, Travis Dudding



PII: S0040-4020(19)31150-0

DOI: <https://doi.org/10.1016/j.tet.2019.130757>

Reference: TET 130757

To appear in: *Tetrahedron*

Received Date: 14 September 2019

Revised Date: 28 October 2019

Accepted Date: 30 October 2019

Please cite this article as: Smajlagic I, Carlson B, Rosano N, Foy H, Dudding T, Charge-enhanced thiourea catalysts as hydrogen bond donors for Friedel–Crafts Alkylations, *Tetrahedron* (2019), doi: <https://doi.org/10.1016/j.tet.2019.130757>.

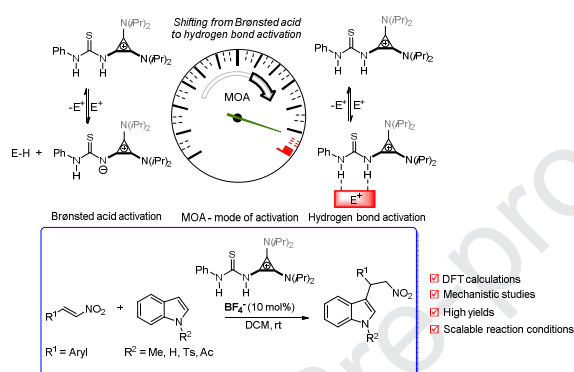
This is a PDF file of an article that has undergone enhancements after acceptance, such as the addition of a cover page and metadata, and formatting for readability, but it is not yet the definitive version of record. This version will undergo additional copyediting, typesetting and review before it is published in its final form, but we are providing this version to give early visibility of the article. Please note that, during the production process, errors may be discovered which could affect the content, and all legal disclaimers that apply to the journal pertain.

© 2019 Published by Elsevier Ltd.

Charge-Enhanced Thiourea Catalysts as Hydrogen Bond Donors for Friedel–Crafts Alkylations

Ivor Smajlagic, Brenden Carlson, Nicholas Rosano, Hayden Foy and Travis Dudding*

Brock University, 1812 Sir Isaac Brock Way, St. Catharines, ON L2S 3A1, Canada.



ABSTRACT Charge-enhanced catalysis has emerged as a powerful alternative to the mainstream use of neutral catalysis.

With this in mind, we report a catalytic Friedel–Crafts alkylation method catalyzed by a charged thiourea incorporating a cationic cyclopropenium moiety. Mechanistic studies, including density functional theory computational calculations, variable time normalization analysis, and ^1H NMR binding studies, collectively reveal this charged-enhanced reactivity proceeds by a dual hydrogen bond-mediated LUMO-lowering mode of substrate activation. Key to these findings is the observed steady-state concentration of the catalyst with *in situ* derived monomeric catalytic species predominating under the reaction conditions.

Keywords: organocatalysis; thiourea; cyclopropenium; Friedel–Crafts alkylation; mechanism; kinetics

INTRODUCTION

Catalysis is a key component of innovative technologies for the production of bulk and fine chemicals.¹ In this regard, metal-free organocatalyzed processes, e.g., hydrogen bond (H-bond) catalysis continues to attract widespread attention as attested for by countless examples over the past two decades.^{2,3} Central to these reports, arguably, and future undertakings is the ability to selectively access one, or more, of these different modes of H-bond activation; however, this is not always a simple task.

One way for accessing a desired mode of H-bond activation is through mechanistic understanding. To this end, various empirical methods and/or physical organic parameters are routinely employed for gaining insight and probing the mechanistic underpinnings of catalysis. In particular, kinetic studies,⁴ determination of pK_a ,⁵ nucleophilicity and electrophilicity parameters,⁶ and colorimetric assays⁷ are often used to provide insight into reaction profiles. Likewise, modern-day computational tools offer a powerful means for acquiring mechanistic understanding and, as such, continue to gain popularity. This is evidenced by numerous reports in drug design,⁸ method development, and material applications.⁹ Further to this point, key in advancing

chemical discovery, more and more, has been the use of density functional theory (DFT) computational calculations as an effective and versatile resource for examining reactivity, e.g., H-bond orchestrated catalyst–substrate interactions and catalysis.¹⁰ The impetus for this development, inherently, being linked to the ability of DFT-guided mechanistic investigations to streamline discovery efforts and circumvent the need for performing laborious experimental screening studies for potential applications.

On a related note, inspired by the many remarkable studies carried out with thiourea catalysts, we recently reported the synthesis and use of cyclopropenium-functionalized cationic thiourea **1** as a Brønsted acid catalyst for synthetically relevant pyranylation of alcohols and phenols¹¹ (Figure 1A, right-hand side). Notably, this catalyst exhibited both cationic H-bond donor and electrostatically enhanced character owing to the cyclopropenium ring system as supported by the computed molecular electrostatic potential (MEP) surface (Figure 1A, left-hand side). Given this precedent, we were intrigued by the prospect of using thiourea **1** as a H-bond catalyst for catalyzing Friedel–Crafts alkylations. In this aim, we envisioned using a DFT-augmented approach to initiate our mechanistic investigation. Realized, this undertaking would add to the

synthetic chemists' toolbox of catalysis and mechanistic understandings, while further demonstrating the utility of modern-day research programs entrenched in computational and experimental chemistries.

Accordingly, we contribute here the first instance of a Friedel–Crafts alkylation catalyzed by a cyclopropenium-based charge-enhanced thiourea organocatalyst. Moreover, this work expands the versatility of cyclopropenium building blocks within another domain of catalysis, namely dual hydrogen bond-mediated catalysis. In terms of practicality, ease of catalyst preparation from inexpensive commercial or readily available reagents in a protecting-group free,¹² operationally simple two-step synthetic route is a salient strength of this method. Further, the heterocyclic indole products furnished by this synthetic approach are prevalent motifs in Nature, such as in natural products offering broad-spectrum bioactivity, e.g., antibacterial, antifungal, and anti-inflammatory properties.¹³ The scalability of this method to gram scales is also demonstrated. Lastly, the computational models reported herein provide in-depth electronic and structural insight we anticipate will aid the future design of thiourea and cyclopropenium/cyclopropenimine catalysts, as well as related chiral organocatalysts.

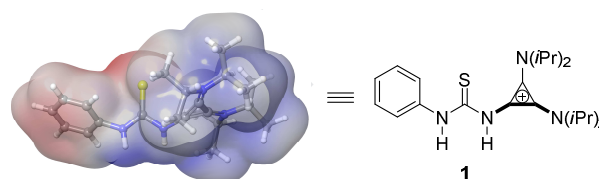
RESULTS AND DISCUSSION

At the outset of this work in targeting the development of Friedel–Crafts alkylation¹⁴ method we were aware the majority of reported organocatalyzed approaches for this transformation were limited by one or more of the following: (1) poor substrate scope (2) use of costly reagents and/or expensive catalyst often prepared by multi-step synthetic routes; (3) lack of scalability; and (4) high catalyst loadings. From these precedents, we postulated our recently reported thiourea catalyst **1** would serve as a viable organocatalyst for Friedel–Crafts alkylation reactions. Central to this proposition was the prospect that cationic thiourea **1** would impart a multifaceted charge-enhanced lowest unoccupied molecular orbital (LUMO)-lowering element of substrate activation. Thus, in keeping with our philosophy of utilizing computation to augment experimental development, we initially turned to DFT to discern to what, if any, extent thiourea **1** would catalyze the Friedel–Crafts alkylation of indoles with Michael acceptor *trans*- β -nitrostyrene (**2a**).

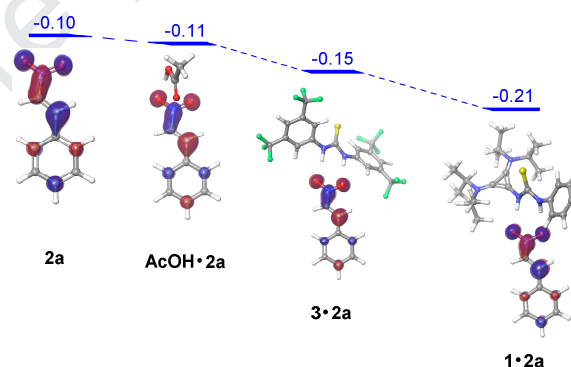
To this end, we performed computational calculations at the (IEFPCM(DCM)) ω B97XD/6-311+G(d,p)/def2-SV// ω B97XD/6-31G(d)/def2-SV level of theory using the Gaussian 09 program (see Supporting Information and Experimental section for computational details) with dichloromethane (DCM) selected as the implicit solvent for these calculations based on the observed solubility of cationic thiourea **1**. Thus, working in the framework of frontier molecular orbital (FMO) analysis the LUMO-lowering activation of *trans*- β -nitrostyrene by **1**, in the absence of a counterion for computational efficiency, was gauged against known Friedel–Crafts alkylation H-bond catalyst *N,N'*-bis[3,5-bis(CF₃)-phenyl]thiourea^{5a,15} (**3**) and acetic acid, which is an ineffective catalyst for this conversion. Most illuminating, cationic thiourea **1** was predicted to have the greatest LUMO-lowering effect as seen by a 0.11 eV reduction in the LUMO energy of substrate **2a**, while the LUMO-lowering effects of thiourea **3** and acetic acid were smaller in magnitude, measuring 0.05 eV and 0.01 eV (see H-bond complexes **Figure 1B**). In terms of the H-bonding manifold of **1**•**2a**, telling, was the presence of a

double H-bond mode of nitro-group binding by the two N–H hydrogen bond acceptor groups of **1** with N–H•••O distances of 1.95 Å and 2.00 Å (**Figure 1C**, left-hand side). These H-bond contacts exhibited characteristic quantum theory of atoms in molecules (QTAIM) bond critical points (BCP) with rho (ρ) densities of 0.023 and 0.025 au and Laplacian ($\nabla^2\rho$) values of -0.021 and -0.023 au, consistent with strong H-bonding.¹⁶ Further, natural bond orbital (NBO) analysis of the donor–acceptor nature of these H-bond interactions, revealed significant charge transfer from the oxygen lone pairs into the antibonding σ^* -orbitals of the N–H bonds ($E_{n\rightarrow\sigma^*} = 17.5 \text{ kcal mol}^{-1}$), hence supporting noticeable charge-transfer-based “partial covalent” H-bonding character (**Figure 1C**, right-hand side).

A Molecular Electrostatic Potential (MEP) Surface



B LUMO Lowering Effect



C H-Bonding Donor–Acceptor Interactions

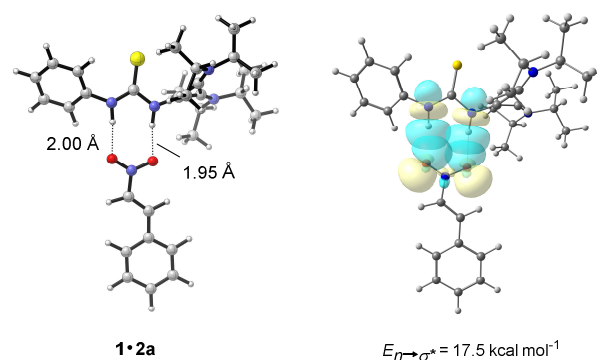
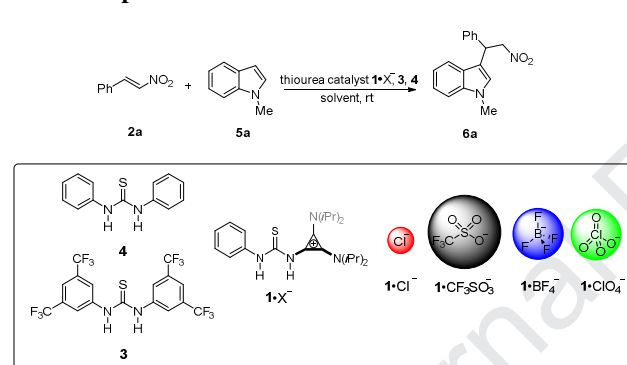


Figure 1. (A) Molecular electrostatic potential (MEP) surface of cationic thiourea catalyst **1**. (B) Computed structures of **2a**, **AcOH**•**2a**, **3**•**2a**, and **1**•**2a** and their respective LUMO energies in electronvolts (eV). (C) H-bonding complex **1**•**2a** (left-hand side) with respective NBO donor–acceptor interactions (right-hand side) (see Supporting Information and Experimental section for computational details).

Charged with this insight, our efforts turned toward the experimental use of thiourea **1** as a H-bond catalyst for Friedel-Crafts alkylation (**Table 1**). In this vein, an initial control reaction performed in the absence of catalyst led to essentially no conversion after 44 hours (entry 1), while sluggish reactivity was observed using neutral thiourea catalysts **3** and **4** (entries 2 and 3). Based on these results and with the aim of improving reactivity, we investigated the use of various charged thiourea catalyst salts of **1**. The logic for doing this being possible tight anion binding, i.e., very short intermolecular N-H...counteranion contacts as a possible source of attenuated reactivity.¹⁷ Corroborating this hypothesis, thiourea **1** with an inexpensive and weakly coordinating tetrafluoroborate counteranion provided superior results relative to **1**•ClO₄⁻, **1**•Cl⁻, and **1**•CF₃SO₃⁻ (entries 4-7). Next, various solvents were screened using thiourea **1**•BF₄⁻ (entries 7-12) resulting in DCM as the solvent of choice affording an optimal conversion of 96% (entry 7). This finding comes as no surprise given solvents with expected H-bond acceptor character are prone to disrupt catalyst-substrate interactions. Lastly, reducing the catalyst loadings to 5 mol% and even as low as 1 mol% attenuated conversion (entries 13 and 14).

Table 1. Optimization of Reaction Conditions^[a]



entry	solvent	catalyst	catalyst load (mol%)	conversion ^[b]
1	CH ₂ Cl ₂	-	-	<5%
2	CH ₂ Cl ₂	4	10	<5%
3	CH ₂ Cl ₂	3	10	34%
4	CH ₂ Cl ₂	1 •ClO ₄ ⁻	10	82%
5	CH ₂ Cl ₂	1 •Cl ⁻	10	10%
6	CH ₂ Cl ₂	1 •CF ₃ SO ₃ ⁻	10	46%
7	CH ₂ Cl ₂	1 •BF ₄ ⁻	10	96%
8	C ₆ H ₅ CH ₃	1 •BF ₄ ⁻	10	64%
9	THF	1 •BF ₄ ⁻	10	36%
10	CHCl ₃	1 •BF ₄ ⁻	10	90%
11	CH ₃ CH ₂ CN	1 •BF ₄ ⁻	10	29%
12	MeCN	1 •BF ₄ ⁻	10	58%
13	CH ₂ Cl ₂	1 •BF ₄ ⁻	5	50%
14	CH ₂ Cl ₂	1 •BF ₄ ⁻	1	18%

^[a]Reactions were performed at room temperature using the following conditions: 0.5 mmol **2a**, 1.5 mmol **5a**, 0.05 mmol catalyst, and 0.5 mL solvent for 44 h. ^[b]Conversion was determined via ¹H NMR spectroscopic analysis of the crude reaction mixtures. This involved monitoring the disappearance of the signal at 8.00 ppm for (**2a**) and appearance of the signal at 5.21 ppm for the FC alkylated product (**6a**).

With optimized reaction conditions in hand, the scope of this reaction with respect to indole was investigated (**Figure 2**). Unprotected indole **5b** reacted with *trans*- β -nitrostyrene to afford product **6b** in very good yield, while *N*-protected indoles¹⁸ **5c** and **5d** resulted in no conversion, presumably, owing to reduced indole nucleophilicity imparted by the electron withdrawing *N*-tosyl and *N*-acetyl groups. Next, we explored the scope of this reaction with respect to the nitroalkene component. Non-functionalized 2-furyl and 2-naphthyl nitroalkenes (**2b** and **2c**) reacted to afford products **6e** and **6f** in good to excellent yields, while electron-rich alkoxy- and alkyl nitroalkenes (**2d-g**) provided variable yields. For instance, *trans*-4-methyl- β -nitrostyrene (**2d**) reacted smoothly to afford product **6g** in excellent yield, whereas alkoxy substituted *trans*- β -nitrostyrenes (**2e-g**) all led to poor conversions (**6h-j**). Further, halogenated *trans*- β -nitrostyrenes (**2h-l**) provided products **6k-o** in good to excellent yields. The high yields of fluorinated products **6k** and electron-poor **6o** is notable given the importance of organofluorine compounds in pharmaceuticals,¹⁹ agrochemicals,²⁰ and material science²¹ industries.

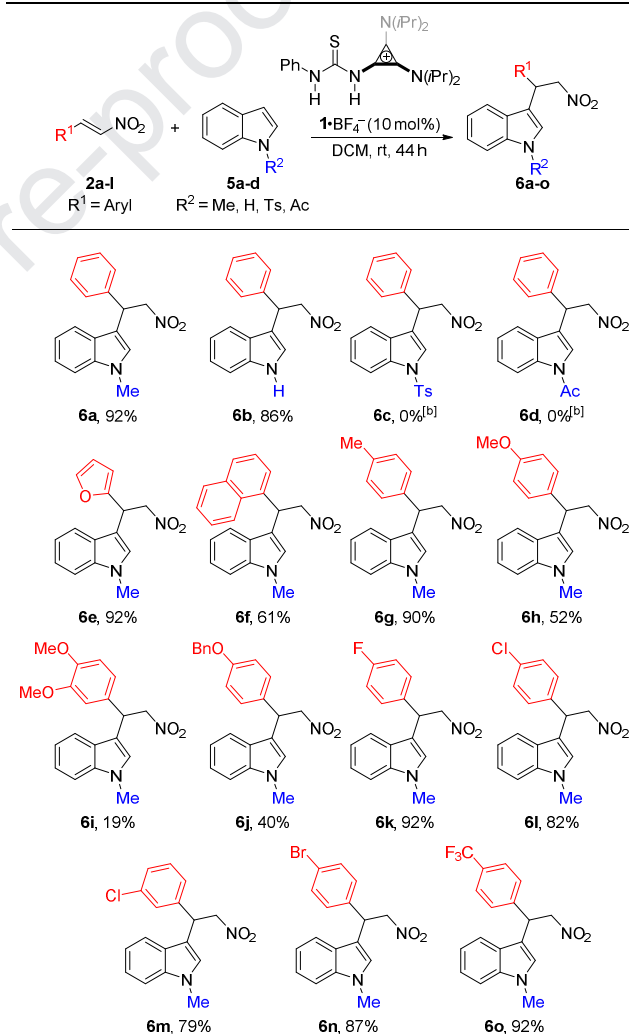


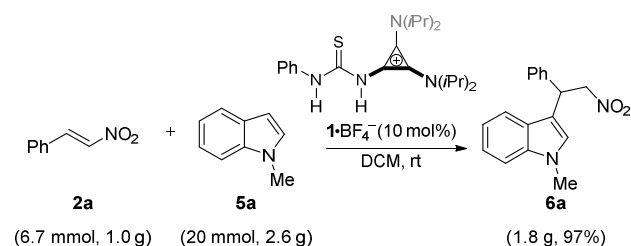
Figure 2. Employment of Thiourea **1•BF₄⁻ for Friedel-Crafts Alkylation**^[a]

^[a]Reactions were performed at room temperature using the following conditions: 0.5 mmol of respective nitroalkene, 1.5 mmol of respective indole, 0.05 mmol **1**•BF₄⁻, and 0.5 mL DCM for 44 h. The yields of isolated products are reported after flash chroma-

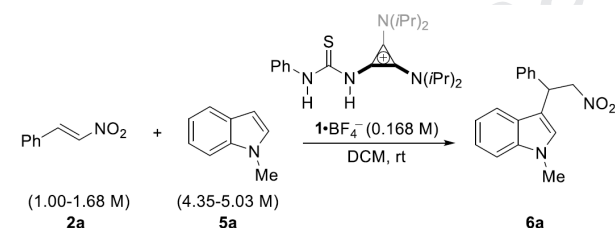
tography. ^[b]No reaction occurred using these *N*-functionalized indoles.

Next, the practicality of this reaction was demonstrated by the gram-scale preparation of Friedel–Crafts alkylation product **6a** in excellent yield (97%, 1.8 g), **Scheme 1**.

Scheme 1. Gram-Scale Reaction Catalyzed by Thiourea **1**•BF₄⁻



Finally, to probe the underlying mechanism of this Friedel–Crafts reactivity and thereby determine the reaction order and stability of catalyst **1**•BF₄⁻, we performed binding studies in conjunction with variable time normalization analysis (VTNA). The latter being a timely qualitative method for extracting mechanistic information from reaction profiles under synthetically relevant conditions.^{4a,22} Addition of increasing equivalents of substrate *trans*- β -nitrostyrene (**2a**) to catalyst **1**•BF₄⁻ in CDCl₃ resulted in a slight downfield shift of the N–H hydrogen atom (¹H NMR, $\Delta\delta = 0.04$ ppm), thus, consistent with a LUMO-lowering mode of substrate activation, as opposed to a Brønsted acid mode of reactivity, see SI. Next, the robustness of the catalyst was probed by a VTNA “same excess” experiment (**Figure 3**).



entry	[2a] (M)	[5a] (M)	[6a] (M)	[1 •BF ₄ ⁻] (M)	[xs]
Expt 1: standard conditions	1.68	5.03	0.00	0.168	0.680
Expt 2: same [xs]	1.00	4.35	0.00	0.168	0.680

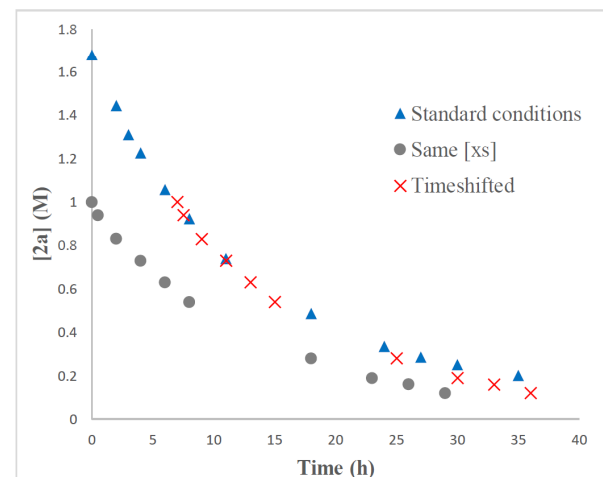


Figure 3. Plot of time (h) vs. concentration (M) for two independent starting concentrations of *trans*- β -nitrostyrene performed under synthetically relevant conditions for the determination of thiourea **1**•BF₄⁻ robustness *via* same excess experiment.

Overlay of the two curves as seen in Figure 3 is telling of steady-state catalyst concentration with catalytic turnover affected by neither catalyst deactivation nor product inhibition (see SI for further details). Further analysis revealed a 0.8-order dependency in catalyst indicative of a high proportion of the catalyst persisting as monomeric species in solution, much unlike that of previous thiourea-catalyzed²³ processes (**Figure 4**). This divergence, presumably, arising from key structural differences, i.e., the bulky cyclopropenium diisopropylamine substituents abating formation of dimeric or higher-order aggregate complexes. Collectively, these kinetic results shed light and speak to the value of incorporating cyclopropenium building blocks as core components of H-bond organocatalysts, such as thiourea catalysts.

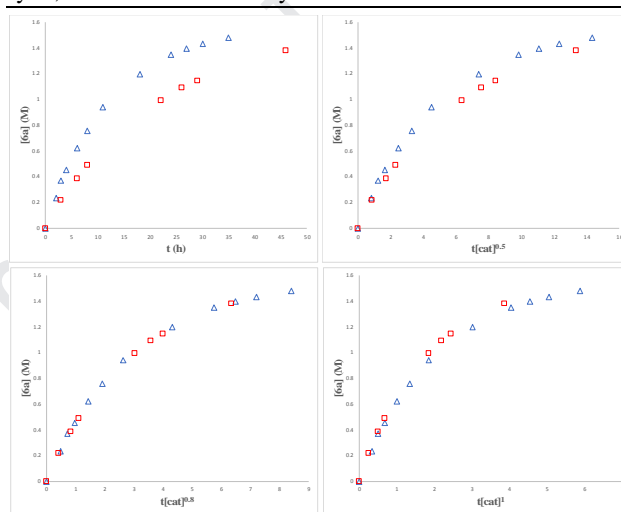


Figure 4. Plot of time (h) vs. concentration (M) for two independent starting concentrations of thiourea **1**•BF₄⁻ (blue triangle - 0.168 M; red square - 0.084 M) performed under synthetically relevant conditions (top left). Plots of normalized time scale ($t[\text{cat}]^{0.5}$) vs. concentration (M) for the determination of the order in catalyst (top right and bottom).

On the basis of the above findings, the tentative DFT supported catalytic cycle depicted in Figure 5 is offered. The cycle initiates in formation of complex **1**•**2a**, which subsequently reacts by rate-determining indole addition transition state **TS1** with a Gibbs free activation energy (ΔG^\ddagger) of 20.5 kcal mol⁻¹ relative to the separate starting reagents and catalyst. Salient features of this transition state include a C···C bond-forming distance of 2.05 Å associated with a synclinal orientation of the styrene and indole substrates as defined by dihedral angle $\theta_{\text{C}(1)\text{-C}(2)\text{-C}(3)\text{-C}(4)}$ measuring -52.1°. Further was a slightly skewed double H-bond manifold with N–H···O distances of 1.84 Å and 1.75 Å linked to a *Z,Z*-thiourea conformation. Though less obvious, was stabilizing charge polarized π - π stacking between the indole ring and the nitroalkene, clearly visible from the green isosurfaces in the non-covalent interaction (NCI) plot of Figure 5. From **TS1** zwitterionic nitronate-azocarbenium intermediate **1**•**6a'** ensues that following a series of proton transfer events leads to exergonic product (**6a**) formation and catalyst turnover.

CONCLUSION

To recap, in building upon the timely relevance of cyclopropenium ions, we have advanced a charge-enhanced cationic thiourea-catalyzed Friedel–Crafts alkylation method. Versatility, scalability, ease of catalyst preparation and operational simplicity are hallmarks of this method. Inherent to the mechanism of these Friedel–Crafts alkylations is a steady-state concentration of a monomeric charged thiourea catalyst, much at odds with existing state-of-the-art reactivity patterns accessible using thiourea catalysts. Additionally, DFT calculations and ^1H NMR binding studies revealed a dual hydrogen bond-mediated LUMO-lowering mode of substrate activation is pivotal to this reactivity. Collectively, the findings of this study provide a compelling basis for the development and future use of cyclopropenium frameworks as charged constructs for enabling catalysis.

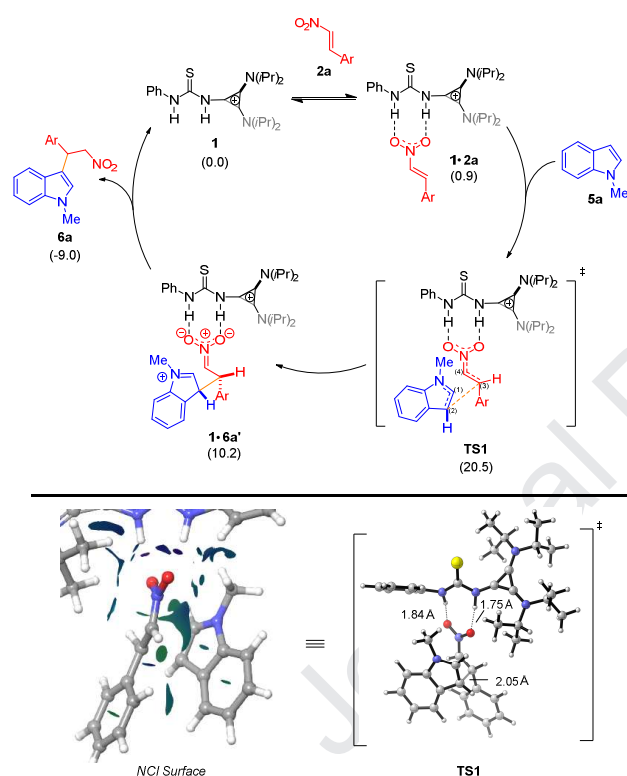


Figure 5. Mechanistic proposal for thiourea-catalyzed (**1**) Friedel–Crafts alkylation. Reported relative Gibbs free energies in kcal mol^{-1} are enclosed in parentheses (see Supporting Information and Experimental section for computational details).

EXPERIMENTAL SECTION

COMPUTATIONAL METHODS

Quantum mechanical calculations were performed using Gaussian 09.²⁴ All geometry optimizations were performed using the ωB97XD functional²⁵ with a 6-31G(d)/def2-SV basis set. The optimized geometries were verified as transition state structures (one imaginary frequency) or minima (zero imaginary frequencies) by frequency calculations. Intrinsic reaction coordinate (IRC) calculations were performed to confirm that all transition state structures were linked to relevant minima. The energies of the $\omega\text{B97XD}/6\text{-}31\text{G(d)}/\text{def2-SV}$ op-

timized structures were further refined by single point calculations performed at the $\omega\text{B97XD}/6\text{-}311+\text{G(d,p)}/\text{def2-SV}$ level of theory using the integral equation formalism polarizable continuum model (IEFPCM) with the default parameters of dichloromethane ($\epsilon = 8.9$) to account for solvent.²⁶ The thermal corrections to the Gibbs free energies (temperature = 298.15 K) computed at the lower level of theory ($\omega\text{B97XD}/6\text{-}31\text{G(d)}/\text{def2-SV}$) were added to the electronic energies obtained from the single point calculations to provide the final reported Gibbs free energies. NBO analysis with program NBO 6 using second-order perturbation theory was used to estimate the contributions of nitro group oxygen lone pair donation into the antibonding σ^* -orbitals of the N–H bonds of cationic thiourea **1**. The 3D images of all optimized geometries were generated with CYLview.²⁷ Natural bond orbital images were produced using Chemcraft.²⁸ GaussView⁵²⁹ was used to construct all structures prior to optimization and to visualize the output from the Gaussian 09 calculations. The program AIM2000³⁰ was used to compute the quantum theory of atoms in molecules (QTAIM) rho (ρ) densities and Laplacian ($\nabla^2\rho$) values at the respective bond critical points (BCP). The reported non-covalent interaction (NCI) plot (isovalue = 0.3, min = -0.05 and max = 0.05), lowest unoccupied molecular orbital (LUMO) diagrams (isovalue = -0.05) and molecular electrostatic potential (MEP) surface (isovalue = 0.001, min = 25.7 and max = 90.4) were calculated using the B3LYP-D3³¹ functional with a LAVP*+ basis set using the program Jaguar of the Schrödinger software package.³²

MATERIALS AND METHODS

Materials were obtained from commercial suppliers and were used without further purification unless otherwise specified. The solvents dichloromethane (DCM), toluene, chloroform, propionitrile, and acetonitrile were distilled using calcium hydride (CaH_2), whereas tetrahydrofuran was distilled from sodium/benzophenone, all under an inert atmosphere (N_2). Reactions were performed under an inert atmosphere in oven-dried glassware. Reactions were monitored by thin layer chromatography (TLC) using TLC silica gel 60 F₂₅₄, EMD Millipore Corporation, and visualized using handheld UV lamps. Flash column chromatography was performed on ultrapure silica gel (230–400 mesh). NMR spectra were obtained with a Bruker DPX-300 (^1H 300 MHz, ^{13}C 75.5 MHz, ^{19}F 292.4 MHz) in CDCl_3 . The observed chemical shifts are reported as δ -values in ppm relative to tetramethylsilane (TMS). Coupling constants (J) are recorded as Hz. Multiplicities are reported as follows: s (singlet), d (doublet), t (triplet), m (multiplet), dd (doublet of doublets), br (broad singlet). Mass spectra were obtained on an MSI/Kratos concept IS mass spectrometer. *trans*- β -nitrostyrene derivatives,³³ catalysts **1**,³⁴ **2**,³⁵ **1**• Cl^- ¹¹ and **1**• BF_4^- ,¹¹ and indole derivatives **5a**,³⁶ **5c**,³⁷ and **5d**³⁸ were prepared according to literature procedures.

N-[2,3-Bis(diisopropylamino)cyclopropenium]-N'-phenylthiourea• ClO_4^- (**1**)• ClO_4^- .

Thiourea **1**• Cl^- (100 mg, 0.24 mmol) was dissolved in DCM (2.00 mL) and washed with saturated bicarbonate (1 x 6.0 mL). The conjugate base was then acidified with a 3 M solution of 70% $\text{HClO}_{4(\text{aq})}$ (1 x 4.0 mL), dried over MgSO_4 and concentrated *in vacuo* to afford a viscous green oil. The oil was then triturated with diethyl ether (2 x 5.0 mL) to furnish thiourea **1**• ClO_4^- as a pale-green solid (98 mg, 85%). Mp: 125–127 °C; ^1H NMR (300 MHz, CDCl_3 , 25 °C): δ = 1.40–1.42 (d, J = 6.8 Hz; 24H), 4.05–4.14 (m, 4H), 7.19–7.24

(t, $J = 7.4$ Hz; 1H), 7.35–7.40 (t, $J = 7.6$ Hz; 2H), 7.75–7.78 (d, $J = 7.8$ Hz; 2H), 9.30 (s, 1H), 9.75 (s, 1H); $^{13}\text{C}\{^1\text{H}\}$ NMR (75.5 MHz, CDCl_3 , 25 °C): $\delta = 21.9, 51.9, 106.2, 123.5, 126.1, 126.4, 128.7, 138.2, 178.1$.

N-[2,3-Bis(diisopropylamino)cyclopropenium]-N'-phenylthiourea• CF_3SO_3^- (**1**)• CF_3SO_3^- .

Thiourea **1**• Cl^- (100 mg, 0.24 mmol) was dissolved in DCM (2.00 mL) and washed with saturated bicarbonate (6.0 mL). The conjugate base was then acidified with a 3 M solution of trifluoromethanesulfonic acid (1 x 2.0 mL), dried over MgSO_4 and concentrated *in vacuo* to afford a viscous green oil. The oil was then triturated with diethyl ether (2 x 5.0 mL) to furnish thiourea **1**• CF_3SO_3^- as a pale-green solid (96 mg, 76%). Mp: 147–149 °C; ^1H NMR (300 MHz, CDCl_3 , 25 °C): $\delta = 1.39$ – 1.41 (d, $J = 6.8$ Hz; 24H), 4.01–4.15 (m, 4H), 7.17–7.22 (t, $J = 7.4$ Hz; 1H), 7.34–7.39 (t, $J = 7.6$ Hz; 2H), 7.77–7.80 (d, $J = 7.9$ Hz; 2H), 9.84 (s, 1H), 10.1 (s, 1H); $^{13}\text{C}\{^1\text{H}\}$ NMR (75.5 MHz, CDCl_3 , 25 °C): $\delta = 21.9, 51.9, 106.6, 123.4, 125.9, 126.8, 128.6, 138.4, 178.3$; $^{19}\text{F}\{^1\text{H}\}$ NMR (292.4 MHz, CDCl_3 , 25 °C) $\delta = -78.3$.

Representative Procedure for the Thiourea-Catalyzed Friedel–Crafts Alkylation.

To an oven-dried 5.0 mL round-bottom flask charged with thiourea **1**• BF_4^- (24 mg, 10 mol%); respective indole (1.5 mmol) and nitroalkene (0.5 mmol) were combined and subsequently diluted in dichloromethane (0.5 mL). The resulting solution was stirred for 44 hours at room temperature under an inert atmosphere. Reaction progress was monitored *via* TLC. After removal of the solvent, the crude material was subjected to flash chromatography using a hexanes/ethyl acetate solvent system to yield the Friedel–Crafts alkylated product.

Characterization Data of the Products (6a-o). NMR data are consistent with the literature.

1-methyl-3-(2-nitro-1-phenylethyl)-1H-indole (**6a**).³⁹

(129 mg, 92%), pink solid. ^1H NMR (300 MHz, CDCl_3 , 25 °C): $\delta = 3.78$ (s, 3H), 4.93–5.00 (dd, $J = 12.3, 8.5$ Hz; 1H), 5.05–5.12 (dd, $J = 12.4, 7.4$ Hz; 1H), 5.19–5.24 (t, $J = 7.9$ Hz; 1H), 6.89 (s, 1H), 7.07–7.13 (t, $J = 6.9$ Hz; 1H), 7.23–7.39 (m, 7H), 7.47–7.49 (d, $J = 7.9$ Hz; 1H).

3-(2-nitro-1-phenylethyl)-1H-indole (**6b**).³⁹

(115 mg, 86%), brown solid. ^1H NMR (300 MHz, CDCl_3 , 25 °C): $\delta = 4.94$ – 5.01 (dd, $J = 12.3, 8.4$ Hz; 1H), 5.06–5.13 (dd, $J = 12.3, 7.6$ Hz; 1H), 5.19–5.25 (t, $J = 7.9$ Hz; 1H), 7.05–7.13 (m, 2H), 7.20–7.39 (m, 7H), 7.46–7.49 (d, $J = 7.9$; 1H), 8.09 (br, 1H).

3-(1-(furan-2-yl)-2-nitroethyl)-1-methyl-1H-indole (**6e**).³⁹

(124 mg, 92%) yellow oil. ^1H NMR (300 MHz, CDCl_3 , 25 °C): $\delta = 3.78$ (s, 3H), 4.91–4.98 (dd, $J = 12.5, 7.4$ Hz; 1H), 5.05–5.12 (dd, $J = 12.5, 8.1$ Hz; 1H), 5.27–5.32 (t, $J = 7.7$ Hz; 1H), 6.22–6.23 (d, $J = 3.3$ Hz; 1H), 6.36–6.37 (dd, $J = 3.1, 1.9$ Hz; 1H), 7.03 (s, 1H), 7.16–7.21 (m, 1H), 7.28–7.38 (m, 1H), 7.43–7.44 (d, $J = 1.1$ Hz; 3H), 7.60–7.62 (d, $J = 7.9$ Hz; 1H).

1-methyl-3-(1-(naphthalen-2-yl)-2-nitroethyl)-1H-indole (**6f**).⁴⁰

(101 mg, 61%) yellow oil. ^1H NMR (300 MHz, CDCl_3 , 25 °C): $\delta = 3.5$ (s, 3H), 5.11–5.14 (dd, $J = 7.4, 1.3$ Hz; 2H), 6.07–6.12 (t, $J = 7.7$ Hz; 1H), 6.86 (s, 1H), 7.07–7.12 (m, 1H), 7.23–7.34 (m, 2H), 7.39–7.60 (m, 5H), 7.80–7.83 (dd, $J = 6.5, 2.8$ Hz; 1H), 7.90–7.93 (m, 1H), 8.27–8.30 (d, $J = 7.9$ Hz; 1H).

1-methyl-3-(2-nitro-1-p-tolyethyl)-1H-indole (**6g**).⁴⁰

(132 mg, 90%) colourless oil. ^1H NMR (300 MHz, CDCl_3 , 25 °C): $\delta = 2.34$ (s, 3H), 3.77 (s, 3H), 4.90–4.97 (dd, $J = 12.4, 8.6$ Hz; 1H), 5.03–5.10 (dd, $J = 12.2, 7.3$ Hz; 1H), 5.17–5.23 (t, $J = 7.9$ Hz; 1H), 6.88 (s, 1H), 7.08–7.17 (m, 3H), 7.22–7.33 (m, 4H), 7.48–7.50 (d, $J = 7.9$ Hz; 1H).

3-(1-(4-methoxy)-2-nitroethyl)-1-methyl-1H-indole (**6h**).⁴⁰

(81 mg, 52%) colourless oil. ^1H NMR (300 MHz, CDCl_3 , 25 °C): $\delta = 3.77$ (s, 3H), 3.82 (s, 3H), 4.93–4.97 (dd, $J = 12.4, 8.6$ Hz; 1H), 5.04–5.11 (dd, $J = 12.3, 7.4$ Hz; 1H), 5.17–5.23 (t, $J = 7.9$ Hz; 1H), 6.91–6.93 (d, $J = 8.7$ Hz; 3H), 7.12–7.18 (m, 1H), 7.28–7.37 (m, 4H), 7.51–7.54 (d, $J = 7.9$ Hz; 1H).

3-(1-(3,4-dimethoxy)-2-nitroethyl)-1-methyl-1H-indole (**6i**).⁴¹

(32 mg, 19%) yellow oil. ^1H NMR (300 MHz, CDCl_3 , 25 °C): $\delta = 3.77$ (s, 3H), 3.85 (s, 3H), 3.88 (s, 3H), 4.89–4.96 (dd, $J = 12.2, 8.6$ Hz; 1H), 5.03–5.09 (dd, $J = 12.2, 7.2$ Hz; 1H), 5.13–5.18 (t, $J = 8.0$ Hz; 1H), 6.83–6.93 (m, 4H), 7.08–7.13 (m, 1H), 7.23–7.34 (m, 2H), 7.48–7.50 (d, $J = 7.9$ Hz; 1H).

3-(1-(4-benzyloxy)-2-nitroethyl)-1-methyl-1H-indole (**6j**).

(77 mg, 40%) colorless oil. ^1H NMR (300 MHz, CDCl_3 , 25 °C): $\delta = 3.77$ (s, 3H), 4.88–4.95 (dd, $J = 12.3, 8.7$ Hz; 1H), 5.03–5.09 (dd, $J = 12.3, 7.8$ Hz; 1H), 5.05 (s, 2H), 5.14–5.20 (t, $J = 7.9$ Hz; 1H), 6.88 (s, 1H), 6.95–6.99 (m, 2H), 7.09–7.14 (m, 1H), 7.24–7.45 (m, 10H); $^{13}\text{C}\{^1\text{H}\}$ NMR (75.5 MHz, CDCl_3 , 25 °C): $\delta = 32.8, 40.9, 70.1, 79.8, 109.5, 113.1, 115.2, 119.1, 119.4, 122.2, 126.3, 126.5, 127.5, 128.0, 128.6, 128.8, 131.7, 136.9, 137.3, 158.2$; HRMS (EI) = m/z : $[\text{M}+\text{H}]^+$ calc'd for $\text{C}_{24}\text{H}_{22}\text{O}_3\text{N}_2$, 386.1636; found: 386.1627.

3-(1-(4-fluorophenyl)-2-nitroethyl)-1-methyl-1H-indole (**6k**).⁴⁰

(137 mg, 92%) yellow oil. ^1H NMR (300 MHz, CDCl_3 , 25 °C): $\delta = 3.78$ (s, 3H), 4.89–4.96 (dd, $J = 12.4, 8.7$ Hz; 1H), 5.04–5.10 (dd, $J = 12.4, 7.2$ Hz; 1H), 5.17–5.23 (t, $J = 7.9$ Hz; 1H), 6.88 (s, 1H), 7.01–7.14 (m, 3H), 7.25–7.36 (m, 4H), 7.43–7.46 (d, $J = 8.0$ Hz; 1H).

3-(1-(4-chlorophenyl)-2-nitroethyl)-1-methyl-1H-indole (**6l**).⁴⁰

(141 mg, 82%) colorless oil. ^1H NMR (300 MHz, CDCl_3 , 25 °C): $\delta = 3.78$ (s, 3H), 4.89–4.96 (dd, $J = 12.5, 8.7$ Hz; 1H), 5.03–5.10 (dd, $J = 12.3, 7.2$ Hz; 1H), 5.17–5.22 (t, $J = 7.8$ Hz; 1H), 6.89 (s, 1H), 7.10–7.16 (m, 1H), 7.26–7.36 (m, 6H), 7.44–7.47 (d, $J = 7.9$ Hz; 1H).

3-(1-(3-chlorophenyl)-2-nitroethyl)-1-methyl-1H-indole (**6m**).⁴⁰

(136 mg, 79%) colorless oil. ^1H NMR (300 MHz, CDCl_3 , 25 °C): $\delta = 3.78$ (s, 3H), 4.88–4.95 (dd, $J = 12.5, 8.6$ Hz; 1H), 5.02–5.09 (dd, $J = 12.6, 7.4$ Hz; 1H), 5.16–5.21 (t, $J = 7.9$ Hz; 1H), 6.90 (s, 1H), 7.09–7.14 (m, 1H), 7.24–7.29 (m, 4H), 7.32–7.35 (m, 2H), 7.44–7.47 (d, $J = 8.0$ Hz; 1H).

3-(1-(4-bromophenyl)-2-nitroethyl)-1-methyl-1H-indole (**6n**).⁴⁰

(156 mg, 87%) colorless oil. ^1H NMR (300 MHz, CDCl_3 , 25 °C): $\delta = 3.79$ (s, 3H), 4.90–4.97 (dd, $J = 12.5, 8.7$ Hz; 1H), 5.03–5.09 (dd, $J = 12.5, 7.2$ Hz; 1H), 5.14–5.20 (t, $J = 7.7$ Hz; 1H), 6.87 (s, 1H), 7.08–7.13 (m, 1H), 7.23–7.34 (m, 4H), 7.42–7.44 (d, $J = 8.0$ Hz; 1H), 7.46–7.49 (dd, $J = 6.6, 1.8$ Hz; 2H).

1-methyl-3-(2-nitro-1-(4-(trifluoromethyl)phenyl)ethyl)-1H-indole (**6o**).³⁹

(160 mg, 92%) yellow oil. ^1H NMR (300 MHz, CDCl_3 , 25 °C): $\delta = 3.79$ (s, 3H), 4.95–5.02 (dd, $J = 12.7, 8.8$ Hz; 1H), 5.07–5.13 (dd, $J = 12.7, 7.2$ Hz; 1H), 5.26–5.31 (t, $J = 7.9$ Hz;

1H), 6.89 (s, 1H), 7.01–7.16 (m, 1H), 7.26–7.36 (m, 2H), 7.40–7.52 (m, 3H), 7.61–7.63 (d, $J = 8.2$ Hz; 2H).

Representative Procedure for Experimental Determination of Potential Product Inhibition or Catalyst Deactivation.

Two separate reactions were conducted in oven-dried 25.0 mL round-bottom flasks charged with 10 mol% catalyst (0.168 M, 0.335 mmol) (**1**•BF₄) to which was added *trans*- β -nitrostyrene (1.68- or 1.00 M; 3.35-, or 2.00 mmol) (**2a**) and 1-methylindole (5.03- or 4.35 M; 10.1- or 8.70 mmol) (**5a**) diluted in 2.0 mL DCM at room temperature under an inert atmosphere. Reaction progress was determined by ¹H NMR (CDCl₃) spectroscopy analyses of aliquots taken periodically. This involved monitoring the disappearance of the signal at 8.00 ppm for (**2a**) and appearance of the signal at 5.21 ppm for the FC alkylated product (**6a**).

Experimental Determination of the Order in Catalyst.

Two separate reactions were conducted in oven-dried 25.0 mL round-bottom flasks charged with either 5- or 10 mol% catalyst (0.084- or 0.168 M; 0.168- or 0.335 mmol) (**1**•BF₄) to which was added *trans*- β -nitrostyrene (1.68 M, 3.35 mmol) (**2a**) and 1-methylindole (5.03 M, 10.1 mmol) (**5a**) diluted in 2.0 mL DCM at room temperature under an inert atmosphere. Reaction progress was determined by ¹H NMR (CDCl₃) spectroscopy analyses of aliquots taken periodically. This involved monitoring the disappearance of the signal at 8.00 ppm for (**2a**) and appearance of the signal at 5.21 ppm for the FC alkylated product (**6a**).

ASSOCIATED CONTENT

The Supporting Information is available free of charge on the ACS Publications website at DOI:

Computational calculations, as well as, kinetic studies and NMR spectra for all reported compounds (PDF)

AUTHOR INFORMATION

Corresponding Author

*E-mail: tdudding@broecku.ca

Author Contributions

The manuscript was written through contributions of all authors. All authors have given approval to the final version of the manuscript.

ORCID

Travis Dudding: 0000-0002-2239-0818

ACKNOWLEDGMENT

Travis Dudding acknowledges financial support from the Natural Science and Engineering Research Council (NSERC) Discovery grant (2019-04205). Computations were carried out using facilities at SHARCNET (Shared Hierarchical Academic Research Computing Network: www.sharcnet.ca) and Compute/Calcul Canada.

REFERENCES

(1) (a) Roberts, S. M.; Poignant, G.; Kozhevnikov, I.; Xiao, J.; Whittall, J.; Pickett, T. E.; Derouane, E. G., Eds.; *Catalysis for Fine Chemical Synthesis*; John Wiley & Sons: NJ, 2004, Vol. 1–5. (b) van Leeuwen, P. W. M. N. *Homogeneous Catalysis: Understanding the Art*; Kluwer: Dordrecht, 2004.

- (2) For timely reviews of organocatalysis, see: (a) Auvil TJ, Schafer AG, Mattson AE. *Eur. J. Org. Chem.* 2014; 2633–2646. (b) Phipps RJ, Hamilton GL, Toste FD. *Nature Chemistry* 2012; 4: 603–614. (c) Giacalone F, Gruttaduria M, Agrigento P, Noto R. *Chem. Soc. Rev.* 2012; 41: 2406–2447. (d) Wende RC, Schreiner PR. *Green Chem.* 2012; 14: 1821–1849. (e) Doyle AG, Jacobsen EN. *Chem. Rev.* 2007; 107: 5713–5743.
- (3) For select reviews on H-bond catalysis and Brønsted acid catalysis, see: Nishikawa Y. *Tetrahedron Lett.* 2018; 59: 216–223. (b) Akiyama T, Mori K. *Chem. Rev.* 2015; 115: 9277–9306.
- (4) (a) Nielsen CD-T, Burés J. *Chem. Sci.* 2019; 10: 348–353. (b) Blackmond DG. *J. Am. Chem. Soc.* 2015; 137: 10852–10866. (c) Blackmond DG. *Angew. Chem. Int. Ed.* 2005; 44: 4302–4320.
- (5) (a) Jakab G, Tancon C, Zhang Z, Lippert KM, Schreiner PR. *Org. Lett.* 2012; 14: 1724–1727. (b) Bordwell FG. *Acc. Chem. Res.* 1988; 21: 456–463.
- (6) Mayr H, Kempf B, Ofial AR. *Acc. Chem. Res.* 2003; 36: 66–77.
- (7) (a) Diemoz KM, Franz AK. *J. Org. Chem.* 2019; 84: 1126–1138. (b) Walvoord RR, Huynh PNH, Kozlowski MC. *J. Am. Chem. Soc.* 2014; 136: 16055–16065. (c) Huynh PNH, Walvoord RR, Kozlowski MC. *J. Am. Chem. Soc.* 2012; 134: 15621–15623.
- (8) (a) Leelananda SP, Lindert S. *Beilstein J. Org. Chem.* 2016; 12: 2694–2718. (b) Sliwoski G, Kothiwal S, Meiler J, Lowe EW Jr. *Pharmacol. Rev.* 2014; 66: 334–395.
- (9) (a) Evans JD, Fraux G, Gaillac R, Kohen D, Trouselet F, Vanson J-M, Coudert F-X. *Chem. Mater.* 2017; 29: 199–212. (b) Butler KT, Frost JM, Skelton JM, Svane KL, Walsh A. *Chem. Soc. Rev.* 2016; 45: 6138–6146.
- (10) For select examples utilizing DFT-augmented approaches, see: (a) Sun Z, Wang Q, Xu Y, Wang ZA. *RSC Adv.* 2015; 5: 84284–84289. (b) Du X, Gao X, Hu W, Yu J, Luo Z, Cen K. *J. Phys. Chem. C* 2014; 118: 13617–13622. (c) Mirabdolbaghi R, Dudding T. *Org. Lett.* 2012; 14: 3748–3751. (d) Rostamikia G, Janik MJ. *Energy Environ. Sci.* 2010; 3: 1262–1274. For reviews, see: Grajciar L, Heard CJ, Bondarenko AA, Polynski MV, Meeprasert J, Pidko EA, Nachtigall P. *Chem. Soc. Rev.* 2018; 47: 8307–8348.
- (11) Smajlagic I, Durán R, Pilkington M, Dudding T. *J. Org. Chem.* 2018; 83: 13973–13980.
- (12) Young IS, Baran PS. *Nature Chemistry* 2009; 1: 193–205.
- (13) For reviews on privileged indole scaffold and applications, see: (a) Xu P-W, Yu J-S, Chen C, Cao Z-Y, Zhou F, Zhou J. *ACS Catal.* 2019; 9: 1820–1882. (b) Ziarani GM, Moradi R, Ahmadi T, Lashgari N. *RSC Adv.* 2018; 8: 12069–12103. (c) Shiri M. *Chem. Rev.* 2012; 112: 3508–3549.
- (14) (a) Herrera RP, Sgarzani V, Bernardi L, Ricci A. *Angew. Chem. Int. Ed.* 2005; 44: 6576–6579. (b) Ganesh M, Seidel D. *J. Am. Chem. Soc.* 2008; 130: 16464–16465.
- (15) (a) Lippert KM, Hof K, Gerbig D, Ley D, Hausmann H, Guenther S, Schreiner PR. *Eur. J. Org. Chem.* 2012; 5919–5927. (b) Schreiner PR, Wittkopp A. *Org. Lett.* 2002; 4: 217–220.
- (16) Grabowski SJ. *Chem. Rev.* 2011; 111: 2597–2625.
- (17) For examples of thiourea catalysts forming ion pair complexes, see: (a) Kennedy CR, Lehnerr D, Rajapaksa NS, Ford DD, Park Y, Jacobsen EN. *J. Am. Chem. Soc.* 2016; 138: 13525–13528. (b) Mittal N, Lippert KM, De CK,

- Klauber EG, Emge TJ, Schreiner PR, Seidel D. *J. Am. Chem. Soc.* 2015; 137: 5748–5758. (c) Berkessel A, Das S, Pekel D, Neudörfl JM. *Angew. Chem. Int. Ed.* 2014; 53: 11660–11664. (d) Lin S, Jacobsen EN. *Nature Chemistry* 2012; 4: 817–824. (e) Xu H, Zuend SJ, Woll MG, Tao Y, Jacobsen EN. *Science* 2010; 327: 986–990. (f) Reisman SE, Doyle AG, Jacobsen EN. *J. Am. Chem. Soc.* 2008; 130: 7198–7199. (g) Taylor MS, Tokunaga N, Jacobsen EN. *Angew. Chem. Int. Ed.* 2005; 44: 6700–6704.
- (18) Song Z, Zhao Y-M, Zhai H. *Org. Lett.* 2011; 13: 6331–6333.
- (19) For reviews, see: a) Müller K, Faeh C, Diederich F. *Science* 2007; 317: 1881–1886. b) Purser S, Moore PR, Swallow S, Gouverneur V. *Chem. Soc. Rev.* 2008; 37: 320–330. c) Wang J, Sánchez-Roselló M, Aceña JL, del Pozo C, Sorochinsky AE, Fustero S, Soloshonok VA, Liu H. *Chem. Rev.* 2014; 114: 2432–2506. d) Kirk KL. *Org. Process Res. Dev.* 2008; 12: 305–321.
- (20) Jeschke P. *ChemBioChem*, 2004; 5: 570–589.
- (21) Hung, M.-H.; Farnham, W. B.; Feiring, A. E.; Rozen S. Functional Fluoromonomers and Fluoropolymers. In: *Fluoropolymers: Synthesis*; Cassidy, P. E., Hougham, G., Johns, K., Davidson, T., Eds.; Kluwert: New York, 1999; Vol. 1, Chapter 4, pp 51–66.
- (22) Burés J. *Angew. Chem. Int. Ed.* 2016; 55: 2028–2031.
- (23) (a) Fan Y, Kass SR. *J. Org. Chem.* 2017; 82: 13288–13296. (b) Fan Y, Kass SR. *Org. Lett.* 2016; 18: 188–191.
- (24) Frisch MJ, Trucks GW, Schlegel HB, Scuseria GE, Robb MA, Cheeseman JR, Scalmani G, Barone V, Mennucci B, Petersson GA, Nakatsuji H, Caricato M, Li X, Hratchian HP, Izmaylov AF, Bloino J, Zheng G, Sonnenberg JL, Hada M, Ehara M, Toyota K, Fukuda R, Hasegawa J, Ishida M, Nakajima T, Honda Y, Kitao O, Nakai H, Vreven T, Montgomery JA Jr, Peralta JE, Ogliaro F, Bearpark M, Heyd JJ, Brothers E, Kudin KN, Staroverov VN, Kobayashi R, Normand J, Raghavachari K, Rendell A, Burant JC, Iyengar SS, Tomasi J, Cossi M, Rega N, Millam JM, Klene M, Knox JE, Cross JB, Bakken V, Adamo C, Jaramillo J, Gomperts R, Stratmann RE, Yazyev O, Austin AJ, Cammi R, Pomelli C, Ochterski JW, Martin RL, Morokuma K, Zakrzewski VG, Voth GA, Salvador P, Dannenberg JJ, Dapprich S, Daniels AD, Farkas O, Foresman JB, Ortiz JV, Cioslowski J, Fox DJ. Gaussian 09, revision D.01; Gaussian, Inc.: Wallingford, CT, 2013.
- (25) Chai J-D, Head-Gordon M. *Phys. Chem. Chem. Phys.* 2008; 10: 6615–6620.
- (26) Cancès E, Mennucci B, Tomasi J. *J. Chem. Phys.* 1997; 107: 3032–3041.
- (27) Legault, C. Y. CYLview, version 1.0b; Université de Sherbrooke: Quebec, Canada, 2009; <http://www.cylview.org>.
- (28) Zhurko, G.; Zhurko, D. ChemCraft, Version 1.8 <http://www.chemcraftprog.com>.
- (29) Dennington, R.; Keith, T.; Millam, J. GaussView, version 5; Semichem Inc.: Shawnee Mission, KS, 2009.
- (30) Biegler-König F, Schönbohm J, Bayles D. *J. Comp. Chem.* 2001; 22: 545–559.
- (31) a) Grimme S. *Wiley Interdiscip. Rev.: Comput. Mol. Sci.* 2011; 1: 211–228. b) Grimme S, Antony J, Ehrlich S, Krieg H. *J. Chem. Phys.* 2010; 132: 154104. c) Grimme S, Ehrlich S, Goerigk L. *J. Comput. Chem.* 2011; 32: 1456–1465.
- (32) a) Schrödinger Release 2018-4: Jaguar, Schrödinger, LLC, New York, NY, 2018; b) Johnson ER, Keinan S, Mori-Sánchez P, Contreras-Garcia J, Cohen AJ, Yang WT. *J. Am. Chem. Soc.* 2010; 132: 6498–6506.
- (33) Worrall DE. *Org. Synth.* 1929; 9: 66.
- (34) Figueiredo J, Serrano JL, Cavalheiro E, Keurulainen L, Yli-Kauhialuoma J, Moreira VM, Ferreira S, Domingues FC, Silvestre S, Almeida P. *Eur. J. Med. Chem.* 2018; 143: 829–842.
- (35) Liedtke T, Spannring P, Riccardi L, Gansäuer A. *Angew. Chem.* 2018; 130: 5100–5104.
- (36) Sha F, Tao Y, Tang C-Y, Zhang F, Wu X-Y. *J. Org. Chem.* 2015; 80: 8122–8133.
- (37) Wang K, Liu Z. *Synth. Commun.* 2010; 40: 144–150.
- (38) Benkovics T, Guzei IA, Tehshik YP. *Angew. Chem. Int. Ed.* 2010; 49: 9153–9157.
- (39) Dong X-W, Liu T, Hu Y-Z, Liu X-Y, Che C-M. *Chem. Commun.* 2013; 49: 7681–7683.
- (40) Huang W-G, Wang H-S, Huang G-B, Wu Y-M, Pan Y-M. *Eur. J. Org. Chem.* 2012; 5839–5843.
- (41) Meshram HM, Rao NN, Kumar GS. *Synth. Commun.* 2010; 40: 3496–3500.

October 28, 2019

Dear Editor,

It is with great pleasure that we submit our manuscript entitled:

Charge-Enhanced Thiourea Catalysts as Hydrogen Bond Donors for Friedel–Crafts Alkylations

*by Ivor Smajlagic, Brenden Carlson, Nicholas Rosano, Hayden Foy and Travis Dudding**

Highlights:

- *The concept of “charge-enhanced acidity” offers insights to improving catalyst activation;*
- *The utility of cyclopropenium frameworks as charged constructs enable catalysis;*
- *The use of variable time normalization analysis (VTNA) as a timely qualitative method in addition to ^1H NMR binding studies probe the underlying mechanism of Friedel–Crafts alkylation reactions;*
- *Computational calculations are powerful tools for acquiring mechanistic insight and directing the development of catalytic methodologies;*

Sincerely,



Professor Travis Dudding
Department of Chemistry, Brock University
St. Catharines, Ontario, L2S 3A1
Office: MC E219, *Phone:* 905-688-5550 x3405
Fax: 905-682-9020, *Email:* tdudding@brocku.ca

Declaration of interests

The authors declare that they have no known competing financial interests or personal relationships that could have appeared to influence the work reported in this paper.

The authors declare the following financial interests/personal relationships which may be considered as potential competing interests: